Product Formation in the Laser Irradiation of Doped Poly(methyl methacrylate) at 248 nm: Implications for Chemical Effects in UV Ablation

ARTICLE *in* THE JOURNAL OF PHYSICAL CHEMISTRY B · JUNE 2004

Impact Factor: 3.3 · DOI: 10.1021/jp031116v

5 AUTHORS, INCLUDING:

Giannis Bounos
Foundation for Research and Technology - H…

26 PUBLICATIONS **219** CITATIONS

SEE PROFILE

Product Formation in the Laser Irradiation of Doped Poly(methyl methacrylate) at 248 nm: Implications for Chemical Effects in UV Ablation

Giannis Bounos, Athanassia Athanassiou, Demetrios Anglos,* Savas Georgiou,* and Costas Fotakis

Institute of Electronic Structure and Laser, Foundation for Research and Technology-Hellas, P.O. Box 1527, 71110 Heraklion, Crete, Greece

Received: September 30, 2003; In Final Form: March 4, 2004

This paper examines the modifications that are induced to photolabile haloaromatic compounds (bromo- and iodonaphthalene, iodophenanthrene, and bromoanthracene) dispersed within poly(methyl methacrylate) (PMMA) films upon irradiation with intense nanosecond laser pulses at 248 nm. To this end, laser-induced fluorescence is employed for the characterization and quantification of the emitting aryl products that remain in the substrate following irradiation. Product formation is examined as a function of laser fluence over 50−2500 mJ cm^{-2}. Employed dopant concentrations are ≤2 wt %, corresponding to absorption coefficients ≤1000 cm^{-1}. At low fluences, ArH-type products are formed via one-photon photolysis of the dopants. However, close to the swelling onset, product formation increases sharply. In parallel, at least in the NapX-doped systems, formation of biaryl species (Nap_2 and perylene) is observed. It is argued that these changes do not result from differences in the excitation/fragmentation of the dopants. They must, instead, reflect differences in the reactivity of the photoproduced radicals. In particular, the increase in ArH product can be ascribed to the enhanced reactivity of the radicals due to the high attained temperatures and heat diffusion to the sublayers. The formation of biaryl species strongly indicates a very low polymer viscosity (≈10^3 Pa s), consistent with transient polymer melting. In fact, biaryl formation provides a direct probe for assessing melting upon laser irradiation. In all, the observations are well accounted for by a thermal model of the laser interaction with PMMA and illustrate the factors that may control reactivity in the UV ablation of polymer substrates.

1. Introduction

UV laser ablation constitutes the basis of a number of diverse techniques aiming at analyzing and processing polymers and other molecular substrates. These include polymer processing in microelectronics,[1−6] matrix-assisted laser desorption of biomolecules,[7−9] deposition of polymeric films,[10] laser processing of tissues,[11,12] and restoration of painted artworks.[13] In all these applications, intense UV laser pulses are employed to irradiate substrates that include a wide variety of chromophores. Generally, the chromophores are photosensitive, dissociating into reactive fragments upon excitation. Thus, minimization of the (photo)chemical effects is crucial for the success of these laser material-processing applications.

From a mechanistic standpoint, the important question that arises is which model is the most appropriate for describing chemical processes in UV ablation. Despite extensive work,[1−5,14] this question remains far from resolved. Product formation in the ablative regime may differ from that at low fluences as a result of alterations in at least one of the following steps: (a) absorption, (b) photolysis (i.e., a change in efficiency), and (c) subsequent fragment/radical reactivity (either due to the high attained temperatures or due to the modified physical condition of the substrate). Elucidation of the relative importance of these factors is necessary for the satisfactory modeling of chemical processes in the UV ablation of polymers and for assessing the validity of models advanced for laser-induced material ejection.

A major obstacle hindering the systematic examination of the above question derives from the chemical complexity of polymers. First, the variety of products that are formed upon UV ablation hampers their thorough experimental characterization. Second, the complexity of the processes, as well as the paucity of information about the photophysics/chemistry of polymers, hinders detailed interpretation of the results. In fact, even the degradation pathways in the irradiation of common polymers at low light irradiances (where the complexities associated with ablation are absent) are yet to be established in detail.[15,16]

To overcome these problems, we focus on the study of polymers doped with relatively simple photosensitive organic compounds (halonaphthalenes, halophenanthrenes, etc). These compounds offer the advantage that their modifications can be probed in detail. Most importantly, their well-known photochemistry provides a basis for the meaningful comparison and evaluation of the chemical effects that are induced in the ablative regime. *Thus, the dopants serve as probes for assessing the changes induced to the polymer upon laser ablation and how these affect chemical reactivity.*

A number of studies have exploited the use of dopants within polymers for probing mechanistic aspects of ablation.[4−5,17] For instance, Dlott and co-workers[18] relied on the use of a specific dye (IR-165) for the direct optical measurement of the temperature developed during ablation of poly(methyl methacrylate) (PMMA) at 1064 nm. A peak surface temperature of ∼600 °C at ablation threshold was estimated. Masuhara and co-workers

* To whom correspondence should be addressed. E-mail: anglos@iesl.forth.gr; sgeorgiu@iesl.forth.gr.

10.1021/jp031116v CCC: $27.50
Published on Web 05/07/2004

have employed aromatic dopants in order to demonstrate the operation of "cyclic" multiphoton processes in the UV ablation of polymers.[19,20] Of direct relevance to the present study is the examination of the decomposition of 5-diazo Meldrum's acid (DM) in the 248 nm ablation of PMMA films doped with this compound.[21] The decomposition yield was determined to be somewhat smaller than unity. The major percentage of the ketene product is formed during the laser pulse and a minor percentage at later times (presumably by thermal decomposition). The ketoketene was indicated to absorb several photons, resulting in efficient heat generation. Lippert and Stoutland examined[22] the decomposition of DM within PMMA films in the irradiation with 266 nm, 60 ps pulses. The ketoketene intermediate was monitored both below and above the threshold by time-resolved infrared spectroscopy. Photolysis of the compound is indicated to be one photon over the examined fluence range. Time-resolved absorption spectroscopy was employed[23] to follow the decomposition of 1,1,3,5-tetraphenylacetone (TPA) within PMMA upon excitation at 266 nm (nanosecond pulses). TPA was found to decompose into two diphenylmethyl radicals and CO. At low fluences, the radical concentration grows linearly with fluence, while at higher fluences, excited radicals are also observed, formed via a two-photon excitation process.

The previous studies seem to indicate that product formation is not modified much with increasing laser fluence. However, the dopants employed in these studies are rather complex molecules that dissociate to stable compounds/fragments (CO or N_2). Their decomposition quantum yield is quite high, with a value close to unity. These features may account for the lack of any significant change as the fluence is raised above the threshold. Furthermore, the studies focused on the early stage of the process ($t_{probing} \approx 1\ \mu s$). However, material ejection and the thermal influence on the substrate are known to last for much longer (microsecond to millisecond).[1,4] Most reactions also take place on this time scale. Thus, though the initial photoexcitation/dissociation steps (depending on the nature of the dopant) may not differ much in the ablative vs sub-ablative regime, considerable deviations can appear in the subsequent dopant reactivity.

Herein, we examine the chemical modifications induced to dopants dispersed within PMMA upon irradiation with intense nanosecond pulses and compare them with those effected at low fluences. To this end, laser-induced fluorescence is employed to characterize the dopant-deriving products formed *in the substrate* following irradiation at 248 nm. Product formation is examined quantitatively as a function of the laser fluence ($50-1500$ mJ cm^{-2}). A number of different halo-aromatics are employed as dopants, namely 1-bromo- and 1-iodonaphthalene, 9-iodophenanthrene, and 9-bromoanthracene (ArX, where Ar = aryl unit; X = I and Br). These compounds undergo a simple homolytic photodissociation to aryl and halogen radicals.[24−26] Thus, as compared to the compounds employed in the previous studies,[19−24] their dissociation and the subsequent radical reactivity is expected to be more sensitive to alterations of the polymer matrix.

We demonstrate that product formation is both qualitatively and quantitatively modified at high laser fluences. At fluences at which polymer "swelling" is induced, formation of ArH products is found to increase sharply. In addition, for the NapX systems, formation of biaryl species (Nap_2 and perylene) is observed at these fluences (for the other examined dopants, formation of biaryls cannot be verified by the employed probing technique). It is argued that these effects do not arise from changes in the excitation/fragmentation step but from differences in the subsequent dynamics of the photoproduced radicals. Specifically, the increase in ArH product can be ascribed to the enhanced reactivity of Ar radicals as a result of the high temperatures attained and heat diffusion to the substrate sublayers. Similarly, the formation of biaryls demonstrates a high diffusivity of the Nap radicals within a high-temperature polymer melt. In all, the results are consistent with a thermal mechanism of 248 nm laser interaction with PMMA. However, subtler factors relating to the changes in the physical condition of the polymer may also affect radical reactivity, but their importance cannot be assessed at present.

The present results are representative of the effects in the irradiation of weakly absorbing systems (≤ 1000 cm^{-1}). It is shown elsewhere that the extent of chemical modifications depends much on the substrate absorptivity at the irradiation wavelength. As indicated in the Discussion, this sensitivity does not relate simply to optical factors (i.e., the different extent of chromophore excitation, but rather they relate mainly to the different relative importance of heat diffusivity to the sublayers vs rate of material removal. The dependence on wavelength will be addressed in detail in a subsequent publication.

2. Experimental Section

Experimentally, the study takes advantage of the fact that the iodoaromatic precursors (ArI) do not fluoresce, whereas the aryl-deriving products are relatively "good" emitters.[24−26] Thus, products can be characterized and quantified via laser-induced fluorescence (LIF). To this end, a Lambda-Physik EMG150 excimer laser is used for irradiation at 248 nm, a Lambda Physik EMG201 for irradiation at 308 nm, and a BMI5011 Nd:YAG laser at 532 nm. The laser beam is focused perpendicularly onto the sample ($\cong(6-10) \times 10^{-2}$ cm^2) via a quartz spherical lens ($f = +50$ cm). After irradiation of the sample with "pump" pulses, product fluorescence is induced by excitation with $F_{LASER} \leq 5$ mJ cm^{-2}. This fluence is low enough to ensure that photolysis by the probe beam is negligible. In all cases, product fluorescence is induced by excitation at 248 nm. For ablation at 248 nm, pumping and probing are effected with exactly the same beam configuration (i.e., the probed area is identical with the ablated one). For "pumping"/irradiation at different wavelengths, the probing 248 nm beam is focused to a size somewhat smaller than the irradiated area. A delay of several seconds between the pump and probe pulses ensures quantitative reaction of the aryl radicals and formation of stable products. Indeed, within the signal-to-noise (S/N) ratio, the product fluorescence intensity remains constant for longer delay times. The main source of error in the measurements derives from the thickness variation across a given sample or different samples (and thus differences in the amount of dopant present). Data presented herein derive from films with a thickness variation of less than 20%.

The induced emission is collected by an optical fiber oriented nearly perpendicularly to the sample at $\sim 1-2$ cm away from its surface (i.e., front-face excitation mode is generally employed). Cutoff filters (<290 nm) are used to minimize detection of laser scattered light. The emission is spectrally analyzed in a 0.20 m grating spectrograph (300 grooves/mm grating) and recorded on an optical multichannel analyzer (OMA III system, EG&G PARC model 1406), interfaced to a computer. For the further characterization of the products, temporally resolved fluorescence spectra are recorded for various detection gates of the OMA.

Irradiation is performed in air. The presence of oxygen may affect the nature of the products (e.g., oxidation of aryl species

TABLE 1: Etching and Swelling Thresholds for the Studied Systems[a]

system (wt)	λ (nm)	absorption coeff. (cm^{-1})[b]	etching threshold (mJ cm^{-2})	swelling "threshold" (mJ cm^{-2})
0.4% NapI/PMMA	248	230	1100	700
1.2% NapI/PMMA	248	450	900	500
0.1% PhenI/PMMA	248	470	800	350
0.5% PhenI/PS	308	≈110	2000	1100

[a] Thresholds determined by profilometric examination of the indicated samples following irradiation with one laser pulse. The error in the thresholds is estimated at ±100 mJ cm^{-2} [b] Absorption coefficients determined from measurements at the indicated laser wavelengths for films cast on suprasil substrates. The absorption coefficient for the neat PMMA at 248 nm is measured, depending on the degree of purification, to be ≈80−150 cm^{-1}. Literature values show an even higher scatter (50 cm^{-1} up to ≈500 cm^{-1}).[5]

to peroxides).[27] Indeed, upon irradiation of ArH/PMMA, the dopant fluorescence is found to decrease with successive laser pulses and/or with increasing fluence. However, since we observe comparable signal decrease in the irradiation of the samples in a vacuum, this decrease is mainly ascribed to thermal desorption of the dopant, as indicated by Fukumura et al.[21] For the ArI-doped systems, there is no specific evidence that O_2 presence affects the aryl products that are formed upon the first laser pulse on virgin surfaces (the focus of this study). At the least, it is of no consequence for the comparison of the products formed above vs those formed below the ablation threshold.

Poly(methyl methacrylate) (Aldrich, average M_w ~120K) and polystyrene (Aldrich, average M_w ~280K) are subjected to extensive purification. Bromo- and iodonaphthalene (Aldrich) are purified by flash chromatography. 1,1-Binaphthyl and perylene (Aldrich) are employed as received. Samples are prepared by casting solutions (in CH_2Cl_2) of the polymer and of the dopant on quartz plates. The samples are dried initially in air and then in vacuo for 24 h. The film thickness is typically in the 10−30 μm range, as measured by profilometer (Diftek).

Surface morphology of the irradiated substrates is examined by profilometry. For the examined, weakly absorbing systems, a fluence range can be delineated in which swelling of the polymer is induced. Ablation, i.e., macroscopic removal of material, is effected at higher fluences. The swelling and etching thresholds determined for the various systems are collected in Table 1.

3. Results

Irradiation of the ArX/PMMA systems (Ar = naphthyl, phenathryl, and anthracyl unit; X = I and Br) with increasing laser fluence results in qualitative and quantitative changes in the dopant-deriving products formed/remaining in the substrate. In the following, we consider first the changes in the product patterns and subsequently the ones concerning their formation efficiency. Since the observations for all examined haloaromatics are largely similar, the presentation details the results on iodonaphthalene, with only the significant differences for the other dopants reported.

3.1. Spectral Characterization of the Dopant-Emitting Products. Figure 1a illustrates LIF probe spectra recorded from NapI/PMMA films with different dopant concentrations after their irradiation with a single pump pulse at *low laser fluences*. In all cases, the probe spectra are dominated by an emission band between 320 and 340 nm (in the case of PhenI, the band appears at ~370 nm—Figure 2). The NapI and PhenI precursors do not fluoresce.[25,26] Furthermore, the indicated band does not

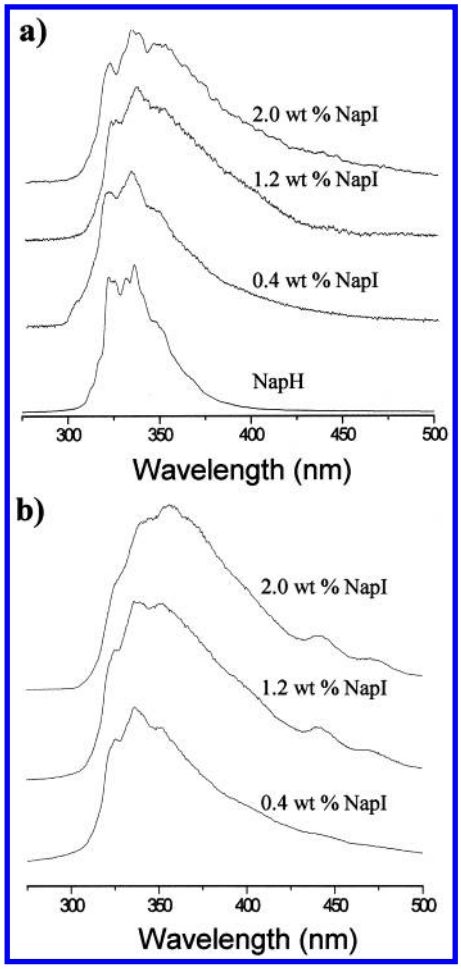

Figure 1. (a) Probe laser-induced fluorescence (LIF) spectra recorded from NapI-doped PMMA samples after their irradiation with a single "pump" pulse at low laser fluence (F_{LASER} = 140 mJ cm^{-2}). For comparison purposes, the spectra have been scaled, and a spectrum recorded from NapH-doped PMMA (0.08 wt %) is also included. (b) Corresponding spectra recorded from the same samples upon the irradiation at $F_{LASER} \approx 1.5$ times the corresponding ablation thresholds.

appear upon irradiation of neat PMMA film. Therefore, this band is due to emitting products deriving from the iodoaromatic dopants.

By comparison with spectra recorded for NapH/PMMA (PhenH/PMMA) films, the band is ascribed to the $^1B_{3u} \rightarrow {}^1A_{1g}$ transition characteristic[25] of NapH (PhenH) and of its substituted derivatives. The temporal emission decay (at λ = 332 nm) is measured to be 100 ± 25 ns, in good correspondence with the known fluorescence lifetime of NapH.[28,29] Analysis of the irradiated samples by GC−MS[30] also indicates NapH to be the main dopant-related product. However, careful examination of Figures 1 and 2 shows that the probe spectra recorded from the haloaromatic (ArX) samples are somewhat less structured than the ArH spectra, thus indicating the formation of additional Ar-substituted products (most likely products of addition of Ar radicals to PMMA). For this reason, we refer to these products as ArH-like. The product(s) of the halogen fragment of the dopant cannot be evidenced in the fluorescence spectra and are not considered further in this study.

With successive laser pulses, the NapH-type emission increases (due to the photolysis of additional dopant molecules) and, in parallel, a broad, structureless band in the 300−500 nm range appears. This band, though less intense, is also observed in the irradiation of neat PMMA films (in this case, the emission

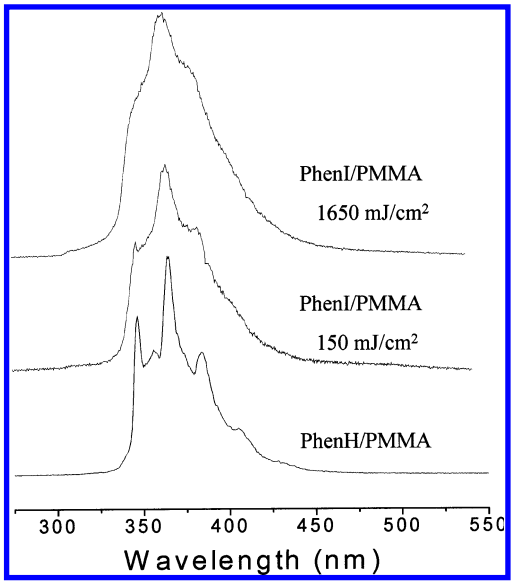

Figure 2. LIF product spectra from 0.1 wt % PhenI-doped PMMA irradiated below and above the ablation threshold ($\lambda = 248$ nm) in comparison with spectrum recorded from PhenH/PMMA (0.08 wt %). The spectra have been scaled.

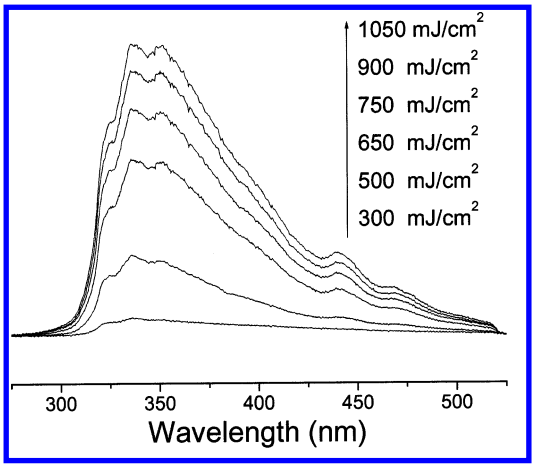

Figure 3. Comparison of the product LIF spectra from 1.2 wt % NapI-doped PMMA film after irradiation with a single laser pulse at increasing 248 nm laser fluences.

is consistent with formation of highly conjugated polymer products, as suggested previously[31−33]). Thus, successive laser pulses result in chemical modifications of PMMA and in ill-defined reactivity between NapI and PMMA species. Due to these complexities, the discussion focuses on the observations following only a single pulse on virgin polymer samples.

Upon irradiation *at higher fluences*, particularly for dopant concentrations ≥1 wt %, the probe spectra recorded after *a single pump pulse* broaden around 370 nm and exhibit, in addition, a double-peak structure around 450 nm (Figure 1b). These features become evident close to the onset of polymer swelling (Table 1). With increasing laser fluence, these emissions grow in intensity until reaching a limiting value at the ablation threshold (Figure 3).

The broadening and the double peak are not observed in the irradiation of NapH-doped films. Consequently, they must be ascribed to (fluorescing) products that are characteristic of the NapBr and NapI reactivity. Species that can be formed in the case of these dopants but not in that of NapH are Nap_2 and related derivatives. The assignment is in very good agreement with the emission spectrum of 1,1-binaphthyl in solution[28,29] and also within PMMA (band centered at 360 nm—Figure 4).

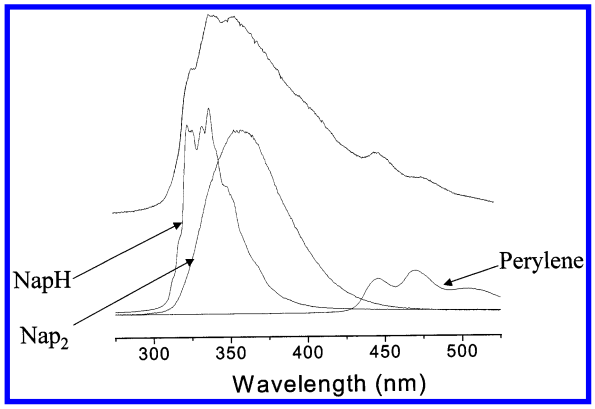

Figure 4. Product LIF spectrum recorded from 1.2 wt % NapI/PMMA following irradiation at high fluences and LIF spectra recorded (under identical conditions, at the probing F_{LASER}) from NapH, Nap_2, and perylene within PMMA. The spectra have been scaled for the purposes of the comparison.

Furthermore, the fluorescence decay (measured at ≈400 nm to minimize NapH-like contributions) is found to be laser-pulse-width limited (≈30 ns), consistent with the very short lifetime reported for Nap_2.[26,29] The double-peak feature is found to be in very good correspondence with the fluorescence spectrum of perylene within PMMA (peaks at $\lambda \approx 440$ and 475 nm)[26] (Figure 4). Perylene can be considered to be a fused Nap_2-type species. Thus, at fluences at which polymer swelling is induced, formation of recombination/condensation products is highly enhanced. Under our probing conditions, the relative sensitivity for NapH (at $\lambda = 332$ nm), Nap_2 (at $\lambda = 370$ nm), and perylene ($\lambda = 450$ nm) is about 1:1.3:3.2. Accordingly, deconvolution of the spectra in Figure 4 indicates that for 1.2 wt % NapI, the relative amount of the corresponding species upon irradiation at high fluences is ≈1:1.2:0.08.

Formation of biaryls is somewhat more pronounced in NapBr/PMMA. In this system, biaryls are detectable for 0.4 wt % samples, whereas for NapI/PMMA, they are clearly discerned at a somewhat higher dopant concentration (≥1 wt %). In the case of PhenI and AnBr, no particular peaks ascribable to biaryl species are discerned. Unfortunately, the fluorescences of $Phen_2$ and An_2 are not well differentiated from those of the corresponding hydrogen-substituted species.[26] Thus, the failure to detect dimer emission for these dopants is inconclusive.

3.2. F_{LASER} -Dependence of Product Formation Efficiency. For the quantitative characterization of the NapH product, the probe fluorescence intensity at $\lambda = 332$ nm, recorded following irradiation of samples with a single pump pulse, is plotted as a function of laser fluence (Figure 5). For the examined dopant concentrations (≤1.2 wt %) and film thickness (10−20 μm), the films are approximately optically thin (absorbance ≈ 0.3−0.4). Thus, at least for laser fluences at which surface morphology is not modified, the fluorescence intensity is proportional to the amount of the aromatic products in the substrate (i.e., no need to correct for self-absorption effects).[34]

At low fluences, the product intensity increases linearly with the pump F_{LASER} (slope in log−log plots generally 1.0 ± 0.2, as determined from 5−6 measurements on each doped system), consistent with a one-photon dissociation of the dopants. However, at higher fluences, the dependence deviates sharply from linearity. The deviation becomes noticeable at fluences at which polymer swelling is detected in the profilometric examination.

Certainly, irradiation at high laser fluences results in an irregular film morphology, with inadvertent effects on the fluorescence measurements. However, the irregular morphology

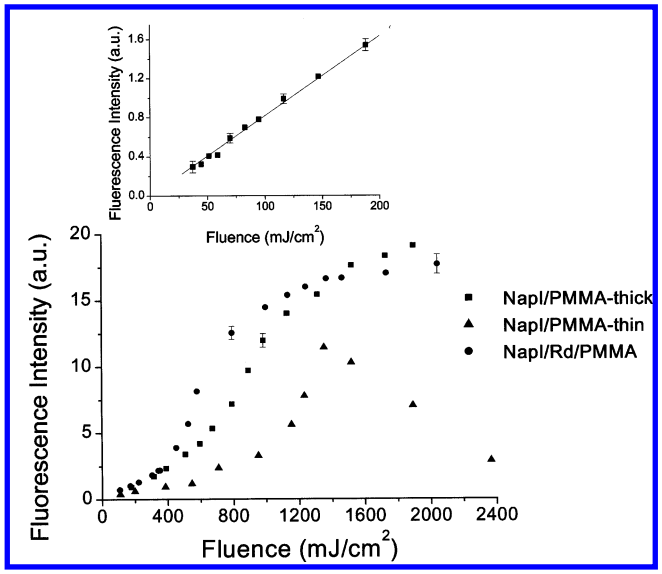

Figure 5. F_{LASER} dependence of the NapH-product intensity upon irradiation of NapI/PMMA (0.4 wt %) with a thickness of ≈8 μm (indicated as "thin"), of NapI/PMMA (0.4 wt %) with ≈20 μm thickness ("thick"), and of Rd/NapI/PMMA (0.1 and 0.4 wt %, respectively; ≈20 μm thick). The fluorescence is recorded following irradiation with a single "pump" pulse at 248 nm. The curves for the NapI/PMMA have been obtained under identical conditions. The dependence of the Rd-doped sample has been normalized at the point recorded at the lowest fluence (since in this case "inner filter" effects invalidate their quantitative comparison). The error bars represent 2σ, as determined from at least five different measurements. The inset illustrates the linear dependence observed for NapH product formation at low laser fluences.

suggests enhanced scattering (i.e., reduced penetration depth) for the probing beam[34] and cannot be responsible for the observed increase of the emission intensity. Indeed, the F_{LASER} dependence is qualitatively independent of probing beam arrangement (e.g., for the probe beam incident from the direction of the substrate, collinearly with the pump beam). In particular, an F_{LASER} dependence similar to that in Figure 5 is obtained for the forward emitted fluorescence. If the increase of the backward emitted fluorescence (i.e., Figure 5) was due to scattering effects, then the forward emitted intensity should correspondingly be reduced (at sharp variance with the experimental results). Furthermore, in the case of 2-naphthyl acetate (within PMMA at 0.5−1 wt %), which is[35] itself fluorescent, whereas its products are not, the F_{LASER} dependence differs markedly from that of Figure 5. For this compound, the fluorescence decreases with increasing laser fluence, reaching a minimum/plateau at the ablation threshold.

In practice, we found that the influence of scattering effects depends on experimental factors, such as the size of the irradiated area and the relative distance of the collecting optical fiber from the substrate.[36] This influence is illustrated by the comparative examination of films with the same dopant concentration but of different thickness (Figure 5, depicting measurements on ≈8 μm vs ≈20 μm thick films). At low fluences, the relative product signal for the two films scales consistently with their thickness. However, at fluences at which the substrate morphology is modified, the ratio of the fluorescence intensities decreases. This indicates that, as a result of scattering effects, the probed depth becomes comparable for the two films. Consequently, the fluorescence measurements may *underestimate* the amount of product formed in the irradiation at high laser fluences. On the basis of various examinations, we estimate that product amount may be underestimated by 15−25%.

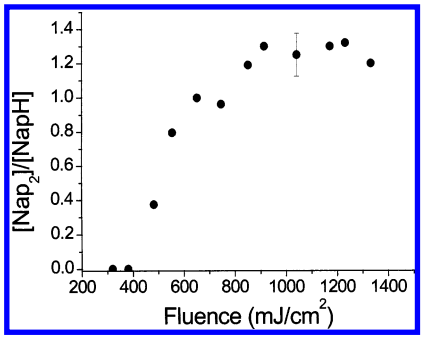

Figure 6. Ratio of Nap_2 vs NapH-like product, as estimated by deconvolution of the spectra, as a function of F_{LASER} in the examination of 1.2 wt % NapI/PMMA. The error bar indicates the likely error in the estimation via the deconvolution procedure.

The same F_{LASER} dependence as that depicted in Figure 5 is obtained for the intensity at $\lambda = 332$ nm, emitted within a temporal window of 100 ± 25 ns (corresponding to the NapH lifetime). Since, for the higher dopant concentrations, the Nap_2 and perylene emissions grow in parallel (Figure 6), the increase in the NapH-like product is not due to its preferential formation over other species. Similar dependences are found for all examined haloaromatics (NapX, X = Br and I; PhenI; and AnBr) at 248 nm, as well as at 308 nm, as long as their concentration is low enough (<2 wt %) for the systems to be weakly absorbing. Furthermore, upon doping of the samples additionally with Rhodamine-6G so as to increase the system absorptivity ($\alpha \approx 470$ cm^{-1}), the ArH product increase is observed at a lower fluence (Figure 5). Therefore, the increase in ArH formation does not relate to specific features (e.g., fragmentation dynamics) of the haloaromatics. Instead, it must relate to effect(s) of the laser irradiation independently of the chromophores involved.

Importantly, a similar dependence is also observed for irradiation of PhenI-doped polystyrene (PS)—concentration of 0.1−0.5 wt %—at 308 nm, i.e., at a wavelength that is weakly absorbed by the system[37] (only PhenI has been examined since its fluorescence can be spectrally differentiated from the PS emission at 320 nm[16]). The similarity of observation for both PMMA and PS, i.e., for two chemically different polymers, shows that the product F_{LASER} dependence in Figure 5 is not characteristic of PMMA reactivity.

Product intensity reaches a plateau at higher fluences. For thick enough films (≥20 mm), the onset of the plateau corresponds nearly to the ablation thresholds of the systems established by profilometry. Thus, ablation results in the leveling off of the product amount remaining in the substrate. At somewhat higher fluences (≥1.5 J cm^{-2}), the intensity of the plasma emission during the ablating pulse is found to increase nearly exponentially with the laser fluence. Thus, at these fluences, plume/plasma shielding[38] as well as scattering[21,39] by bubbles, voids, etc. in the substrate limits the pump intensity in the substrate and the induced photochemical modifications.

4. Discussion

The present study has examined the (emitting) aryl products formed in the 248 nm irradiation of ArX-doped (Ar = NapX, X = Br and I; PhenI; and AnBr) PMMA at high fluences and compared them with the corresponding ones at low fluences. Because the study probes the species that remain in the substrate, the effects can be analyzed free from the complications (i.e., secondary absorption and fragmentation, plasma formation, etc.) that plague the analysis of the gas-phase ejected species. The

main observations concerning the chemical effects induced at high laser irradiances can be summarized as follows: (a) a sharp increase in the amount of the aryl-deriving (ArH-type) products that remain in the substrate and (b) at least for the NapX dopants, an efficient formation of Nap_2 and higher-order/fused aromatic condensates (perylene). These results demonstrate that dopant reactivity is qualitatively and quantitatively modified from that at low laser fluences. In the following, we rely on the known photophysics/chemistry of the dopants to account for these changes and to establish the factors that affect reactivity in UV ablation.

Concerning the observations at low fluences ($\leq$200 mJ cm^{-2}), these can be directly accounted for. Upon excitation at $\leq$266 nm in both gas phase and solution, ArX dissociates efficiently into Ar and X radicals (for iodo derivatives, quantum yield of photolysis is $\approx$1 and $\approx$0.8 for bromo derivatives).[25,26] At these fluences, photolysis is a one-photon process, as clearly shown by the linear F_{LASER} dependence of the ArH product emission (inset in Figure 5). Furthermore, for NapI and PhenI, given their very rapid dissociation ($\approx$1 ps),[25] product formation via direct reactions of excited states can be ruled out (this possibility cannot be fully discounted for the bromo derivatives, which have a longer excited-state lifetime).[25] A percentage of the Ar radicals may abstract a hydrogen atom from PMMA to form ArH.[40] Products may also form via addition reactions of the radical to PMMA chains.[41]

Within this framework, we consider next the implications of the observations for dopant reactivity upon irradiation at high laser fluences. In fact, the F_{LASER} dependence of Figure 5 directly indicates shortcomings of phenomenological ablation models. In particular, the so-called "layer-by-layer" or "blow-off" model,[1,12] usually employed to describe material etching with nanosecond laser pulses, assumes

$$l_{ejected} = 1/\alpha \ln(F_{LASER}/F_{thr}), \quad \text{for } F \geq F_{thr} \qquad (1)$$

(where $l_{ejected}$ represents the etching depth and α is the (effective) absorption coefficient), i.e., the substrate below the ejected layer is subject to a constant F_{thr}. According to the assumptions underlying the formula,[1,4,12] the photoproduct amount would be expected to scale with F_{LASER}, leveling off at the ablation threshold. Of course, several limitations of this model have been acknowledged.[4] For instance, below the ablation threshold, desorption of volatile products may occur;[4,5,14] swelling is observed in the irradiation of weakly absorbing polymers.[4,19,20] Thus, it is not surprising that deviations from the expected F_{LASER} dependence of product formation are noted already at fluences below the threshold. On the other hand, once the threshold is reached, the prediction for a nearly constant product amount in the substrate seems to be born out (observation of a plateau at the higher fluences in Figure 5). Here, any additional radicals/products formed with increasing laser fluence are evidently removed by the etching process. Even so, the extent of product formation at the plateau is much higher than that predicted by eq 1.

Concerning the enhanced ArH-like product formation, three factors can in principle be responsible: (a) changes in the absorption process (e.g., saturation or multiphoton processes), (b) enhanced thermal decomposition of the dopant, and (c) changes in the subsequent reactivity of the photogenerated aryl radicals

Concerning possibility (a), it is important that the increase in ArH is observed for a film thickness as low as 5$-$10 μm (i.e., much smaller than the linear optical penetration depth). Therefore, it is not due to an increase of depth over which photoproducts are formed. This, for example, would the case be if absorption process were saturated.[50] Instead, there is an enhancement in product formation per unit volume.

The increase in ArH cannot be ascribed to an enhancement in the photodegradation of ArX. In the ablation of C_6H_5Cl-doped PMMA, Dickinson and Lippert have suggested[45,46] that material preheating by the early part of the pulse may increase the dissociation yield of the excited molecules. For the highly photolabile ArI (dissociation yield $\approx$1), this possibility is not important. Multiphoton excitation/dissociation can be similarly discounted. Fluences in excess of 5 J cm^{-2} are required for a two-photon process to compete with ArI dissociation (assuming an absorption cross-section for the secondary step equal to that for C_6H_6[27] and related compounds). Thus, even at high laser fluences, ArI dissociation must proceed via a one-photon excitation.

We note that this conclusion does not exclude the possibility of (cyclic) multiphoton processes suggested by Masuhara, Fukumura,[19$-$21] and co-workers. In fact, reaching temperatures sufficient to induce PMMA decomposition at the fluences reported in Table 1 requires that the effective absorption coefficient during the pump pulse must be $\geq$1000 cm^{-1} (in comparison, for 0.4 wt % NapI/PMMA, the small signal absorption value would suggest temperatures of only 360 and 450 K at swelling and etching thresholds, respectively). It is likely that the aryl radicals formed by ArX photolysis absorb additional photons, similarly to what is indicated for the diazo-doped system.[21] Note that as a result of such multiphoton processes, even direct transmission measurements of the ablating pulse cannot establish the one-photon nature of photofragmentation of the ArX precursors. Yet, despite the operation of such processes reducing the effective optical penetration depth, ArH product formation is found to increase rather than decrease.

As a second possibility, enhanced thermal decomposition of ArX may be presumed. Initial studies of the translational distributions of species ejected upon ablation claimed temperatures as high as 3000 K.[47$-$49] However, it is now clear that these values overestimate film temperatures, due to the severe collisional perturbation of the desorbate translational features in the plume. In the IR ablation of doped PMMA, Dlott and co-workers estimate the temperature to be $\approx$870 K at the threshold, reaching a "ceiling" value of $\approx$990 K at high fluences (due to the steep rise of the polymer heat capacity with increasing temperature).[50]

Energy removal by material ejection is significant on the microsecond time scale.[50] Subsequent cooling due to thermal diffusion is estimated to last some milliseconds (see below). Assuming the activation energy for the C$-$I bond scission to be equal to the 2.6 eV bond energy[26] (i.e., no activation barrier) and a rather high pre-exponential factor of 10^{13} s^{-1}, only 10^{-6} ArX is estimated to decompose on microsecond and $\sim 10^{-3}$ on millisecond time scales. To discount further the possibility of thermal decomposition, we examined product formation in the 532 nm ablation of NapI/Rd/PMMA, where Rd = Rhodamine-6G (concentration, 1 wt %). At this wavelength, absorption is due exclusively to the rhodamine dopant ($\epsilon \approx 1.05 \times 10^5$ M^{-1} cm^{-1}).[27] Even for irradiation at fluences as high as 2 J cm^{-2} and for NapI concentrations as high as 4 wt %, no NapH emission is detected (within the S/N ratio) when the irradiated areas are subsequently probed at 248 nm. It is reasonable to assume that the temperatures that develop in the ablation of this system are comparable to those in the irradiation of ArI/PMMA at 248 nm. Therefore, ArI thermal decomposition is not significant under the employed irradiation conditions.

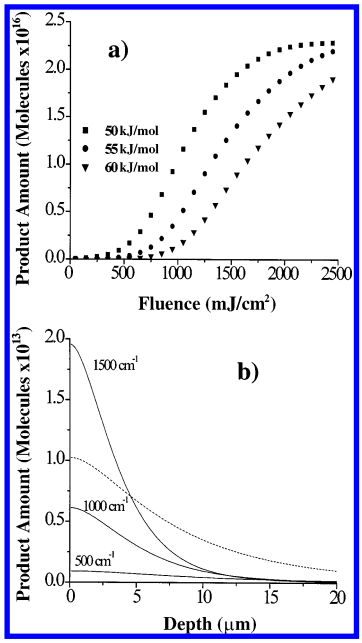

Figure 7. (a) Total product estimated to form as a function of laser fluence for different E_{act} of the Nap radicals reaction ($\alpha_{NapI/PMMA} \approx 150$ cm^{-1}, $\alpha_{eff} \approx 1000$ cm^{-1}, 20 μm). (b) NapH product as a function of depth for different effective absorption coefficients ($t = 1$ ms after the laser pulse, $F_{LASER} = 0.50$ J cm^{-2}). The dotted line represents the product distribution for the effective absorption coefficient of 1000 cm^{-1} and $t = 5$ ms.

The previous result does not exclude, of course, the possibility that the "thermal component" does not affect the subsequent reactivity of the photogenerated Ar radicals. To model this effect, we assume temperature evolution in the substrate to be given by[51,52]

$$T(z,t) = T_0 + \frac{\alpha_{eff}F_{LASER}}{2C_P}\exp(\alpha_{eff}^2 D_{th}t)\left[\exp(-\alpha_{eff}z)\,\mathrm{erfc}\left(\alpha_{eff}\sqrt{D_{th}t} - \frac{z}{2\sqrt{D_{th}t}}\right) + \exp(\alpha_{eff}z)\,\mathrm{erfc}\left(\alpha_{eff}\sqrt{D_{th}t} + \frac{z}{2\sqrt{D_{th}t}}\right)\right] \quad (2)$$

where z is the depth from the film surface (erfc, complementary error function). The formula neglects energy removal by desorption of volatile species (sub-ablative regime) or by material ejection (ablation). $T_0 = 300$ K and for PMMA, $\rho = 1.19 \times 10^3$ kg m^{-3}, $C_p = 2 \times 10^3$ J kg^{-1} K^{-1} (25−250 °C) growing to $\approx 3 \times 10^3$ J kg^{-1} K^{-1} at higher temperatures, and $D_{th} = 4 \times 10^{-8}$ m^2 s^{-1}.[50] The effective absorption coefficient α_{eff} is fixed, as indicated above, in order to attain the substrate temperatures estimated in previous studies.[50] For the H-abstraction by Ar radicals, a pseudo-unimolecular process is assumed, with an activation barrier in the range of 30−60 kJ mol^{-1} and a 10^8 pre-exponential factor[53] (unfortunately, accurate literature values for these reactions are lacking to permit a quantitative comparison). For the simulation, the substrate is divided in slabs, and product formation is integrated over time.

Despite the uncertainties in the effective absorption coefficient and the reaction rate constants, the predicted F_{LASER} dependence reproduces qualitatively the experimental value (for $E_{act} \approx 50$ kJ mol^{-1}, a reasonable value for such reactions) (Figure 7a). The simulation affords the following explanation for the observed dependence. At low laser fluences, only a small percentage of the photoproduced Ar radicals are estimated to react to ArH products. In this case, the nonreacted Ar radicals probably recombine eventually with the geminate halogen radical (experimentally indicated to represent ≈80% of the photoexcited molecules).[54] With increasing laser fluence, the percentage of reacting radicals increases sharply. Even in the case of a decrease of the optical penetration depth (i.e., operation of multiphoton processes), the reduction in the extent of photolysis is overcompensated by the number of reacting Ar radicals, due to the enhanced temperature rise. Due to heat diffusing from the upper layers, a much higher percentage of Ar radicals in the underlying layers of the substrate reacts to ArH or aryl-substituted polymer (Figure 7b). Consequently, the reaction should be limited by the heat relaxation time $\tau \approx 1/(\alpha_{eff}^2 D_{th}) \approx 10^{-3}-10^{-2}$ s, and the effective "reaction depth" can be approximated as

$$\sqrt{(1/\alpha_{eff}^2)\ln\left[\frac{(\alpha_{eff}F_{LASER}/\rho C_P)[\ln A - \ln(a_{eff}^2 D_{th})]}{(E_{act}/R)}\right]} \approx 7-15\ \mu\mathrm{m}$$

where A and E_{act} represent, respectively, the preexponential factor and the activation energy of the reaction (Figure 7b).

Close to the ablation threshold, the use of eq 2 fails. At these fluences, energy removal by material ejection, as well as the sharp increase in C_p, should limit the attained temperatures, thereby resulting in the leveling off of product formation in the remaining substrate. Yet, the finding that the product amount at the plateau is much higher than predicted by eq 1 suggests that, in these weakly absorbing systems, the velocity of surface recession in the ablative regime remains too low to compete with heat diffusion to the sublayers, resulting in product formation.[43]

The thermal model can be further quantified by the observations on Nap_2 formation. First, it is noted that the possibility of Nap_2 formation within pre-existing film NapI aggregates can be rejected. No bands besides that of NapI are detectable in the UV spectra of the samples. In NapH/PMMA, we detect excimer emission (at ≈400 nm)[27] at much higher concentrations (>10−12 wt %) than those employed for NapI. Furthermore, if Nap_2 and perylene were formed within pre-existing aggregates, then they should also be observed in the irradiation at low laser fluences. However, in the absence of morphological changes to the substrate, these species are not observed, even for dopant concentrations as high as 2 wt % (Figure 1a). Finally, no Nap_2 or perylene emission could be detected during the pump pulse, further arguing against their direct (expected to be quite fast) formation within aggregates. In all, for the examined NapI concentrations (<2 wt %), dopant aggregation cannot account for the Nap_2 formation.

In view of this conclusion, Nap_2 and perylene must form via diffusion-limited reactions, i.e.,

$$\mathrm{Nap} + \mathrm{Nap} \rightarrow \mathrm{Nap_2\ or\ perylene}$$

In support of a bimolecular process, the intensities of these species grow supralinearly with F_{LASER} (and thus, the number of radicals produced) and NapX (X = Br and I) concentration.[55] The operation of such reactions directly indicates a very high radical "mobility" at these fluences. Even at the highest examined concentration, the average distance between dopant molecules is ≈4 nm. Assuming Fickian-type diffusion,[57] $r = 2(Dt)^{1/2}$, D must be $\approx 10^{-12}$ m^2 s^{-1} for Nap_2 formation on microsecond and $\approx 10^{-15}$ m^2 s^{-1} on millisecond time scales. From $D = k_B T/6\pi\eta R$ (where k_B is the Boltzmann constant, η is

the medium viscosity, and R is the naphthalene radius) and assuming T in the range of 500−1000 K for the indicated time interval(s), η is estimated to be $\approx 10^1-10^3$ Pa s, comparable to or even higher than the viscosity values reported for polymer *melts*.[56,57] Thus, the observation of Nap_2 formation close to the swelling onset supports the suggestion[39] that this corresponds to PMMA melting.

In fact, the extent of binaphthyl formation also depends on the efficiency of the competing abstraction reactions. Since reactivity of aryl radicals for H-abstraction increases sharply with temperature (e.g., as observed[58] for C_6H_5 radicals), the largest percentage of the Nap radicals may react to form NapH before they have the chance to encounter one another. Thus, the D values above underestimate species mobility. This high mobility has been implicitly assumed in a number of previous studies.[20−22,59−62] Recently, Tokarev et al.[61,62] have employed micropatterning schemes for obtaining quantitative evidence of transient liquid microflow in the UV ablation of polymers. The present results demonstrate the importance of this transient phase change for the induced chemical effects. In particular, the formation of the biaryl species provides a direct experimental probe for assessing "diffusion" within polymers during laser irradiation. For instance, as described elsewhere, the Nap_2 yield differs much for ablation at 308, 248, and 193 nm, plausibly indicative of the different "melt depths" due to the different absorptivity of the systems at these wavelengths.[63] On the other hand, no Nap_2 is detected upon ablation of the same systems with subpicosecond pulses (248 nm, 500 fs).[64]

In all, the observations are well accounted for by a thermal model for the 248 nm irradiation of ArX-doped PMMA. It is noted that according to such a model (more precisely, the so-called "bulk photothermal model"[14,43]), material ejection is determined by the breakage of a critical number of bonds. Consequently, the extent of heat dissipation to the substrate, and thus its influence on product formation, will depend on the polymer molecular weight (MW). MW determines the number of bonds needed to be broken and therefore the efficiency of material ejection and energy removal. As a result, product patterns differ somewhat according to MW (a lower NapH-like and Nap_2 formation are observed for low MW PMMA).[65] In this respect, the PMMA of 120K amu studied here represents an intermediate system.

Finally, though the observations have been explained exclusively in terms of the temperature evolution, there may be additional, subtler factors involved. It is interesting that for both PMMA (at 248 and 308 nm) and PS (at 308 nm), the deviation of the ArH product formation from linearity is most pronounced close to the swelling onset. Furthermore, Nap_2 formation becomes clearly noticeable at this fluence. Plausibly, this correspondence reflects the influence of the increase in polymer-free volume that accompanies swelling. Photolysis yields (at low laser fluences) of photolabile compounds within polymer glasses are generally much smaller than those in solution.[16,66] This difference has been ascribed to the constraining effect of the polymer matrix that promotes radical recombination. Generally, the rate of geminate radical separation is a strong function of viscosity, η (in liquids, approximately proportional to $\sqrt{T/\eta}$).[67] In view of the high decrease of η that is indicated by Nap_2 formation, a corresponding increase in radical separation efficiency can be expected, with a consequent increase in ArH formation. Thus, in addition to the temperature factor, alterations in the physical condition (state) of the polymer may affect product formation. The quantification of the importance of this possibility requires a systematic study of different polymers characterized by different glass and melting points.

5. Conclusions

In contrast to most studies aimed at establishing the mechanisms of material ejection, the present one has focused on examining how chemical effects differ in the ablative vs subablative regime. To this end, we have examined the modifications induced in haloaromatic, ArX (Ar, Nap, Phen, and An; X = Br and I), dopants dispersed within PMMA upon UV irradiation (248 and 308 nm). The aryl products remaining in the substrate have been probed as a function of laser fluence.

For these weakly absorbing systems ($\alpha < 1000$ cm^{-1}), irradiation at high fluences is found to result in a sharp increase of the ArH-like product and in the formation of biaryl species (the latter unambiguously identified in the case of the NapX (X = Br and I) dopants). Clearly, chemical processes deviate from those induced at low laser fluences. Changes in the absorption and fragmentation fail to account for these observations. Instead, they must reflect changes in the reactivity of the photoproduced Ar radicals. In particular, the increase in ArH product can be ascribed to the development of high temperatures, resulting in a higher percentage of the Ar radicals reacting than that at low laser fluences. Furthermore, the formation of biaryls demonstrates a very high radical mobility, consistent with transient melting of the polymer at these fluences. In all, the results can be well accounted for within a thermal model of the 248 nm laser interaction with PMMA.

In all, the systematic examination of products as a function of laser fluence reveals detailed information about the chemical effects induced in ablation, even for extensively studied systems, such as PMMA. Such studies can provide a basis for the guided optimization of the laser processing schemes of molecular substrates. Furthermore, they can be useful in assessing the relative validity of the models that have been advanced for describing laser-induced material ejection.

Acknowledgment. The authors thank Dr. N. Bityurin for useful discussions and suggestions. This work was supported in part by the Ultraviolet Laser Facility operating at F.O.R.T.H. under the Improving Human Potential (IHP)-Access to Research Infrastructures program (contract no. HPRI-CT-1999-00074), by the Training and Mobility of Researchers (TMR) program of the EU (project no. ERBFMRX-CT98-0188), and by the PENED program (project no. 01EΔ 419) of the General Secretariat of Research and Technology−Ministry of Development (Greece).

References and Notes

(1) Srinivasan, R.; Braren, B. *Chem. Rev.* **1989**, *89*, 1303.
(2) *Photochemical Processing of Electronic Materials*; Boyd, I. A., Ed.; Academic Press: London, 1992.
(3) *Laser Ablation. Principles and Applications*; Miller, J. C., Ed.; Springer Series in Materials Science 28; Springer-Verlag: Berlin, 1994.
(4) Bäuerle, D. *Laser Processing and Chemistry*; Springer-Verlag: Berlin, 2000.
(5) Lippert, T. J.; Dickinson, T. *Chem. Rev.* **2003**, *103*, 453.
(6) Georgiou, S.; Hillenkamp, F. *Chem. Rev.* **2003**, *103*, 317.
(7) Karas, M.; Hillenkamp, F. *Anal. Chem.* **1989**, *59*, 2299.
(8) Tanaka, K.; Waki, H.; Ido, Y.; Akita, S.; Yoshida, Y.; Yoshida, T. *Rapid Commun. Mass Spectrom.* **1988**, *2*, 151.
(9) Vertes, A.; Gijbels, R. In *Laser Ionization Mass Analysis*; Vertes, A., Gijbels, R., Adams, F., Eds.; John Wiley: New York, 1993; p 127.
(10) Chrisey, D. B.; Pique, A.; McGill, R. A.; Horwitz, J. S.; Ringeisen, B. R.; Bubb, D. M.; Wu, P. K. *Chem. Rev.* **2003**, *103*, 553.
(11) . *Laser-Tissue Interaction IX*; Jacques, S. L., Ed.; SPIE Proceedings Series 3254; SPIE: Bellingham, WA, 1998.
(12) Vogel, A.; Venugopalan, V. *Chem. Rev.* **2003**, *103*, 577.
(13) (a) Georgiou, S.; Zafiropulos, V.; Anglos, D.; Balas, C.; Tornari, V.; Fotakis, C. *Appl. Surf. Sci.* **1998**, *127−129*, 738. (b) Kautek, W.;

Pentzien, S.; Rudolph, P.; Krüger, J.; König, E. *Appl. Surf. Sci.* **1998**, *127−129*, 746. (c) Oujja, M.; Rebollar, E.; Castillejo, M. *Appl. Surf. Sci.* **2003**, *211*, 128.

(14) Bityurin, N.; Luk'yanchuk, B. S.; Hong, M. H.; Chong, C. T *Chem. Rev.* **2003**, *103*, 519.

(15) Rabek, J. F. *Mechanisms of Photophysical Processes and Photochemical Reactions in Polymers: Theory and Applications*; John Wiley: Chichester, 1987.

(16) Schuabel, W. *Polymer degradation*; Carl Hanser Verlag Publishers: Munich, 1981.

(17) Lippert, T.; Yabe, A.; Wokaun, A. *Adv. Mater.* **1997**, *9*, 105.

(18) Hare, D. E.; Dlott, D. D. *Appl. Phys. Lett.* **1994**, *64*, 715.

(19) Furutani, H.; Fukumura, H.; Masuhara, H. *J. Phys. Chem.* **1996**, *100*, 6871.

(20) Fukumura, H.; Mibuka, N.; Eura, S.; Masuhara, H.; Nishi, N. *J. Phys. Chem.* **1993**, *97*, 13761.

(21) Fujiwara, H.; Fukumura, H.; Nakajima, Y.; Masuhara, H. *J. Phys. Chem.* **1995**, *99*, 11481 and references therein.

(22) Lippert, T.; Stoutland, P. O. *Appl. Surf. Sci.* **1997**, *109/110*, 43.

(23) Arnold, B. R.; Scaiano, J. C. *Macromolecules* **1992**, *25*, 1582.

(24) Haselbach, E.; Rohner, Y.; Suppan, P. *Helv. Chim. Acta* **1990**, *73*, 1644.

(25) Dzvonik, M.; Yang, S.; Bersohn, R. *J. Chem. Phys.* **1974**, *61*, 4408.

(26) Birks, J. B. *Photophysics of Aromatic Molecules*; John Wiley & Sons: London, 1970.

(27) Twarowski, A. J.; Dao, P. J. *J. Phys. Chem.* **1988**, *92*, 5292.

(28) Offen, H. W.; Beardslee, R. A. *J. Chem. Phys.* **1968**, *48*, 3584.

(29) Canonica S.; Wild, U. P. *J. Phys. Chem.* **1991**, *95*, 6535.

(30) Products from irradiated (raster-scanned) films were extracted in hexane and analyzed on a Shimadzu GC17A gas chromatograph, with a Supelco SBP-5 fused silica capillary, coupled with a Shimadzu GCMS-QP 5050 mass-selective detector (70 eV nominal ionization energy).

(31) Larciprete, R.; Stuke, M. *Appl. Phys. B: Lasers Opt.* **1987**, *42*, 181.

(32) Krajnovich, D. J. *J. Phys. Chem. A* **1997**, *101*, 2033.

(33) Blanchet, G. C.; Cotts, P.; Fincher, C. R., Jr. *J. Appl. Phys.* **2000**, *88*, 2975.

(34) (a) Ishimaru, A. *Propagation and Scattering in Random Media*; Academic: Orlando, 1978; Vol. 1. (b) Ying, J.; Liu, F.; Alfano, R. R. *Appl. Opt.* **1999**, *38*, 224.

(35) Wang, Z.; Holden, D. A.; McCourt, F. R. W. *Macromolecules* **1990**, *23*, 3773.

(36) Attempts to quantify this influence through the use of fluorescing organic dopants proved unsuccessful because all tested compounds were found to be photochemically unstable or to desorb at these laser fluences.

(37) Tsunewaka, M.; Nishio, S.; Sato, H. *Jpn. J. Appl. Phys., Part 1* **1995**, *34*, 218.

(38) Lazare, S.; Granier V. *J. Appl. Phys.* **1988**, *63*, 2110.

(39) Furutani, H.; Fukumura, H.; Masuhara, H. *J. Phys. Chem.* **1996**, *100*, 6871.

(40) *Handbook of Organic Photochemistry*; Scaiano, J. C., Ed.; CRC Press: Boca Raton, FL, 1989; Vol. II.

(41) For Ar-substituted PMMA products, the fluorescence yields should be comparable, independent of the polymer chain size, so that changes in product distribution may not affect the total product fluorescence intensity much. At any rate, as shown, the influence of ablation/temperature increase on radical reactivity is so pronounced that differences in the product distribution are of secondary importance.

(42) Tucker, S. A.; Griffin, J. M.; Acree, W. E.; Zander, M.; Mitchell, R. H. *Appl. Spectrosc.* **1994**, *48*, 458.

(43) (a) Arnold, N.; Bityurin, N. *Appl. Phys. A: Mater. Sci. Process.* **1999**, *68*, 615. (b) Bityurin, N.; Arnold, N.; Luk'yanchuk, B.; Bäuerle, D. *Appl. Phys. A: Mater. Sci. Process.* **1998**, *127−129*, 164.

(44) (a) Ediger, M. N.; Pettit, G. H. *J. Appl. Phys.* **1992**, *71*, 3510; (b) Pettit, G. H.; Ediger, M. N.; Hahn, D. W.; Brinson, B. E.; Sauerbrey, R. *Appl. Phys. A: Mater. Sci. Process.* **1994**, *58*, 573.

(45) Webb, R. L.; Langford, S. C.; Dickinson, J. T.; Lippert, T. K. *Appl. Surf. Sci.* **1998**, *127−129*, 815.

(46) Lippert, T.; Webb, R. L.; Langford, S. C.; Dickinson, J. T. *J. Appl. Phys.* **1999**, *85*, 1838.

(47) Koren, G. *Appl. Phys. B: Lasers Opt.* **1998**, *46*, 147−149.

(48) Davis, G. M.; Gower, M. C.; Fotakis, C.; Efthimiopoulos, T.; Argyrakis, P. *Appl. Phys. A: Mater. Sci. Process.* **1985**, *36*, 27.

(49) Srinivasan, R.; Braren, B.; Dreyfus, R. W.; Handel, L.; Seeger, D. E. *J. Opt. Soc. Am. B* **1986**, *3*, 785.

(50) (a) Chen, S.; Lee, I.-Y. S.; Tolbert, W. A.; Wen, X.; Dlott, D. D. *J. Phys. Chem.* **1992**, *96*, 7178. (b) Lee, I.-Y. S.; Wen, X.; Tolbert, W. A.; Dlott, D. D.; Doxtader, M.; Arnold, D. R. *J. Appl. Phys.* **1992**, *72*, 2440.

(51) (a) Brunco, D. P.; Thompson, M. O.; Otis, C. E.; Doodwin, P. M. *J. Appl. Phys.* **1992**, *72*, 4344. (b) Cain, S. R.; Burns, F. C.; Otis, C. E. *J. Appl. Phys.* **1992**, *71*, 4107.

(52) Babu, S. V.; Couto, G. C.; Egitto, F. D. *J. Appl. Phys.* **1992**, *72*, 692.

(53) Scaiano, J. C.; Stewart, L. C. *J. Appl. Phys.* **1983**, *105*, 3609.

(54) The estimation is based on the measurement of the number of laser pulses necessary for the complete photolysis of ArI within PMMA at low laser fluences (50−100 mJ cm^{-2}). The main error is introduced by the parallel increase in the substrate absorptivity, due to the accumulation of Ar-deriving and PMMA decomposition products. Thus, the condition of the optically thin sample is not satisfied after extensive irradiation.

(55) The dependence on concentration may not follow the expected second-order law because a change in the NapI concentration affects, in parallel, the amount of absorbed energy and thus the extent of thermal decomposition of the polymer.

(56) El-Sayed, F. E.; MacCallum, J. R.; Pomery, P. J.; Shepherd, T. M. *J. Chem. Soc., Faraday Trans. 2* **1979**, *75*, 79.

(57) Haward, R. N.; Young, R. J. *The Physics of Glassy Polymers*; Champand & Hall: London, 1997.

(58) Park, J.; Chakraborthy, D.; Bhusari, D. M.; Lin, M. C. *J. Phys. Chem. A* **1999**, *103*, 4002.

(59) Beinhorn, F.; Ihlemann, J.; Luther, K.; Troe, J. *Appl. Phys. A: Mater. Sci. Process.* **1999**, *68*, 709.

(60) Schmidt, H.; Ihlemann, J.; Wolff-Rottke, B.; Luther K.; Troe, J. *J. Appl. Phys.* **1998**, *83*, 5458.

(61) Tokarev, V. N.; Kaplan, A. F. H. *J. Appl. Phys.* **1999**, *86*, 2836.

(62) Weisbuch, F.; Tokarev, V. N.; Lazare, S.; Debarre, D. *Appl. Phys. A: Mater. Sci. Process.* **2003**, *76*, 613.

(63) Athanassiou, A.; Andreou, E.; Fragouli, D.; Anglos, D.; Georgiou, S.; Fotakis, C. *J. Photochem. Photobiol., A* **2001**, *145*, 229.

(64) Lassithiotaki, M.; Athanassiou, A.; Anglos, D.; Georgiou, S.; Fotakis, C. *Appl. Phys. A: Mater. Sci. Process.* **1999**, *69*, 363.

(65) Bounos, G.; Georgiou, S., unpublished results.

(66) Strictly speaking, the term "cage effects" refers to the promotion of recombination. Here, we include the possibility that below the threshold, NapH fluorescence may be quenched by the counterpart, I (i.e., external heavy atom effect). For the purposes of this study, this "looser" use of the term is immaterial.

(67) Noyes, R. M. *Prog. React. Kinet.* **1961**, *1*, 29.